Composite-hydroxide-mediated approach an effective synthesis route for BaTiO₃ functional nanomaterials

Taj Muhammad Khan[1,2] · M. Zakria[1] · Rana. I. Shakoor[1] · Shabbir Hussain[3]

Abstract This paper describes synthesis of the functional BaTiO₃ (BT) nanostructures by composite-hydroxide-mediated (CHM) approach. The effect of processing temperature on the nucleation and the optical, structural properties is investigated. The nanostructures prepared at various temperatures (180, 220 and 250 °C) are thermally stable and nucleate in different morphologies, which shows a temperature-dependent mechanism of the CHM approach. The nanostructures are cubic in nature with an average particle size in the range of 97–250 nm. The local crystal structure investigated by Raman spectroscopy reveals a certain degree of tetragonality on atomic scale in the local phase structure. The micrographs of scanning electron microscopy (SEM) indicate formation of the nanocuboids at 180 and 220 °C with larger particle size. At 250 °C, the product shows ball-like spherical morphology. Energy-dispersive X-ray (EDX) confirms the existence of Ba, Ti and O elements in the product, which indicates a chemically pure product. Further signature on the formation, purity and chemical bonding is obtained from FT-IR spectroscopy. Based on these experimental results, size, morphology manipulation and possible growth mechanisms are proposed with CHM at low temperature and without surfactant.

✉ Taj Muhammad Khan
  tajakashne@gmail.com

1 National Institute of Lasers and Optronics (NILOP), P.O. Nilore, Islamabad 45650, Pakistan

2 School of physics, Trinity College Dublin (TCD), Dublin 2, Ireland

3 Pakistan Institute of Nuclear Science and Technology (PINSTECH), P.O. Nilore, Islamabad 45650, Pakistan

1 Introduction

Perovskite (ABO₃) materials are of great significance and scientific interest because of its ferroelectric, piezoelectric and thermoelectric properties [1]. They have a wide range of potential applications, such as ferroelectric random access memory (FRAM), piezoelectric transducers, solid-oxide fuel cells, superconductors, thermoelectrics, ferromagnets, high-capacitance capacitors, pyroelectric detectors and magneto-resistors [1, 2]. Among these materials, BaTiO₃ has high dielectric constant and ferroelectric properties. Therefore, it is extensively used in multilayer ceramic capacitors (MCC), nonlinear optics, gate dielectrics, modulators, actuators and IR detectors. Bulk BaTiO₃ has the classical ABO₃ (Ba²⁺ as A and Ti⁴⁺ as B) perovskite structure. The ferroelectric and dielectric properties of these nanomaterials are correlated with the size of nanocrystals. Nowadays, the technological trend toward miniaturization of optoelectronic devices makes it of great interest to examine this correlation when sizes are at the nanoscale. In this way, it is scientifically fascinating and technologically challenging to synthesize and characterize a nanosized barium titanate (BT) nanostructure (nanowires, nanoparticles) [3–5]. Furthermore, device miniaturization and high permittivity can be achieved by controlling the microstructure which strongly depends on the composition, homogeneity, surface area and size of the particle. To manufacture reliable MCC, a highly pure, well-crystalline, agglomerate-free and superfine ceramics are required [6]. Recently, there has been an improved research in nanoscale particles because their physical properties are strongly depending on the particle size, and crystalline structure, which could be controlled through the synthesis parameters.

BT nanoparticles are produced by variety of synthesis techniques such as solid-state reaction [7], hydrothermal
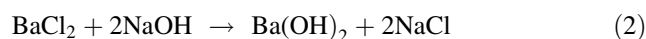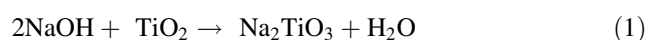
process [8] and solvothermal process [9]. For these processes, various synthesis parameters are optimized and controlled to obtain BT nanomaterials. However, the proposed CHM approach is one of the synthesis techniques seems technically sound, environment-friendly, cost-effective, and a versatile method to produce a wide range of nanostructures. Recently this technique was used by Khan et al. for the CdO and ZnO nanostructures [10, 11]. In this method, a few parameters including growth temperature and reaction time are required to control. Further, this method works at low temperatures and without surfactants. The environmental appeal of this technique comes from its intrinsic scalability, generality, nontoxic and one-step process. The fundamental basis of this method is on the utilization of hydroxide melts as a reaction medium [12]. The BT nanoparticles have also been studied by Miao et al. [13] using CHM approach. This study is very limited and describes only one growth temperature of 220 °C, while viscosity shows a significant effect on the morphological structure of the product at higher temperatures beyond 200 °C. To see this effect, synthesis at higher temperatures is necessary to conduct. Moreover, extensive study requires including spectroscopic properties by Raman and IR which are complement methods and shows a degree of significant for probing nanostructures.

In this research article, we have studied CHM approach for the synthesis of BT nanomaterials at various growth temperatures in the range of 180–250 °C for the same reaction time (48 h) and formation of the nanomaterials is characterized. Thermal stability and optoelectronic properties of the produced nanostructures are investigated, and a temperature-dependent mechanism is proposed. For better understanding the size manipulation, morphological and spectroscopic properties, we have examined the crystal structure, size, shape, chemical nature and morphology by the methods of X-ray diffraction (XRD), Raman spectroscopy, FT-IR and scanning electron microscopy (SEM). The morphology and particle sizes are also described in terms of the viscosity of the melts used in the synthesis.

2 Materials and characterization

Perovskite $BaTiO_3$ nanomaterials were synthesized by composite-hydroxide-mediated (CHM) approach. The synthesis method has been described in our early reports [10, 11]. A 10 g of mixed hydroxides (NaOH/KOH = 51.5:48.5) was placed in a 50-mL Teflon vessel. During the chemical reactions, hydroxides play a double role, as solvent and as a reactant to decrease the synthesis temperature. A mixture of anhydrous $BaCl_2$ and TiO_2 of 0.5 mmol each was used as the raw materials for the chemical reactions. The raw material was added on the top of the hydroxides in the vessel. We have divided the total composite mixture into three samples, and each of these samples was placed into a 25-mL Teflon vessel separately. Each vessel was then put in a furnace and preheated to 180 °C followed by repeated experiments at 220, and 250 °C for a constant reaction times of 48 h. After the hydroxides were totally molten, the molten hydroxides were mixed uniformly by shaking the vessel to ensure uniformly mixed reactants, and the vessel was put back into the furnace. After reacting for 48 h, the vessel was taken out and cooled to room temperature. The solid product was filtered and washed first by deionized water and then with hot water to remove hydroxides on the surface of the particles. The complete preparation steps of BT nanomaterials by CHM method has been illustrated in Fig. 1. The mechanism of chemical reactions using CHM approach for the synthesis of BT nanoparticles is as under,

$$2NaOH + TiO_2 \rightarrow Na_2TiO_3 + H_2O \qquad (1)$$

$$BaCl_2 + 2NaOH \rightarrow Ba(OH)_2 + 2NaCl \qquad (2)$$

$$Na_2TiO_3 + Ba(OH)_2 \rightarrow BaTiO_3\downarrow + 2NaOH. \qquad (3)$$

The structural properties of the prepared $BaTiO_3$ product were examined by X-ray diffractometer with CuKα radiation of wavelength $\lambda = 1.5405$Å. X-ray diffraction (XRD) measurements were taken in the 2θ range of 10–75°. The surface morphology and elemental composition were investigated by the methods of scanning electron microscopy (SEM) and energy-dispersive X-ray (EDX). The chemical bonding was analyzed by NICOLET 6700 Fourier Transform Infrared spectroscopy (FT-IR). The Raman spectra were obtained at room temperature with a Raman spectrograph (MST-4000A, DONGWOO OPTRON, CO., Ltd.) using multichannel air-cooled (−50 °C) charged coupled device (CCD) and an excitation source: a He-Cd laser emitting at wavelength 441.6 nm and operated at power 80 mW. The laser power on the sample was not measured. The spectra were obtained in the spectral range of 200–1200 cm^{-1} with a spectral resolution of 4 cm^{-1}. The data acquisition was made for 5 s and with an exposure time of 10 s using INDOR software.

3 Results and discussions

3.1 XRD analysis

X-ray diffraction (XRD) pattern of BT nanomaterials is shown in Fig. 2. XRD analysis shows a polycrystalline behavior of $BaTiO_3$ with cubic perovskite crystal structure. The nanocrystals have preferred orientation along (001) plane. From the pattern, it is quite evident that there is no split in the (200) peak around 45° due to minimum distortion in the crystal structure and change in the symmetry

Fig. 1 Illustration of preparation steps for the synthesis of BT nanostructures by CHM method
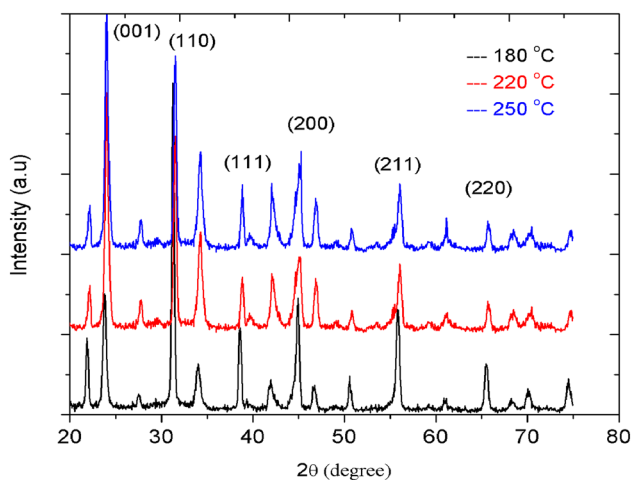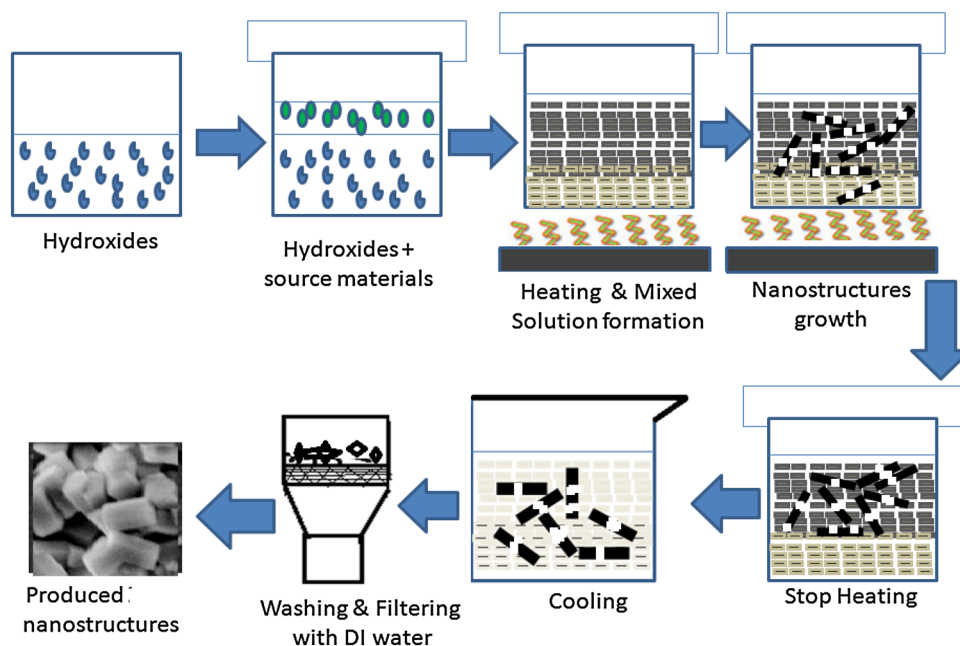
Fig. 2 XRD pattern of the as-prepared $BaTiO_3$ nanoparticles prepared via CHM approach at processing temperatures: 180, 220 and 250 °C

of the BT nanoparticles. This implies that the structure of the product nanomaterials is cubic. The lattice constant (a) for the nanoparticles is about 4.127 Å and cell volume V, 70.291 Å³, which are in good agreement with the literature values for the cubic $BaTiO_3$ (JCPDS card No. 75-0215) [14]. The average particle size of BT nanoparticles is estimated from the (110) reflection peak using the Debye–Scherer's formula [15]. The (110) peak in the XRD graph for both the samples corresponds to a particle size of ~ 75 nm and FWHM of 0.18° with no significant differences between the three samples. However, intensity of the (110) peak is larger at 220 and 250 °C compared to 180 °C,

which implies the crystallinity improves at higher synthesis temperatures. The cubic phase does not change with synthesis temperature, which means a thermodynamically stable phase. Intensities of the (110) and (001) reflections change at 220 °C, which indicates nanocrystals are re-oriented at this growth temperature and the highest growth of the nanoparticles is in the (110) direction. A decrease in broadening and asymmetric behavior of the (200) peak around ($2\theta \sim 45°$) for the samples prepared at 220 and 250 °C reveals that tetragonality in the structure has decreased and a cubic nature appeared in the product. This change is well consisted with Raman investigation for the BT nanomaterials [16]. The analysis of Raman and XRD shows a complexity in the phase transition of $BaTiO_3$, with order–disorder as well as displacive character [17].

3.2 Raman spectroscopy studies

Raman spectroscopy is a highly sensitive and important optical technique to characterize nanomaterials regarding structural symmetry. XRD measurements elucidate the average and static symmetries, while Raman scattering can easily clarify the local and dynamic symmetries. This is because ferroelectric properties are closely related to lattice dynamics and Raman spectroscopy provides a valuable measuring method on the samples to further supplement our XRD results.

From the XRD analysis, BT has a cubic perovskite structure; however, by performing Raman analysis on the product, the observed Raman active modes imply a certain degree of tetragonality on the atomic scale. $BaTiO_3$ cubic nanoparticles intrinsically have no Raman active modes;
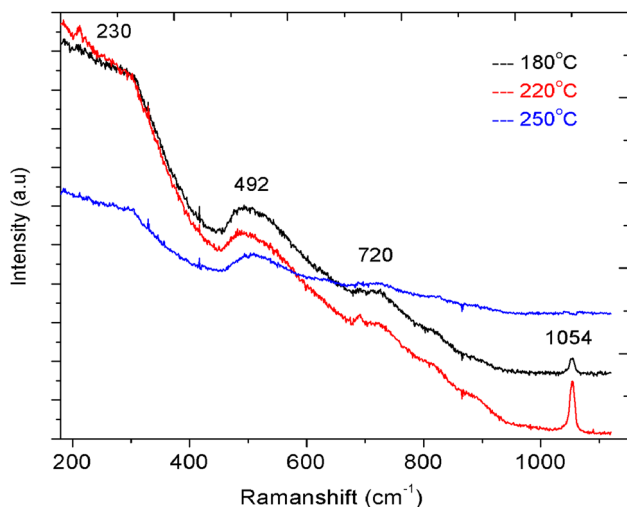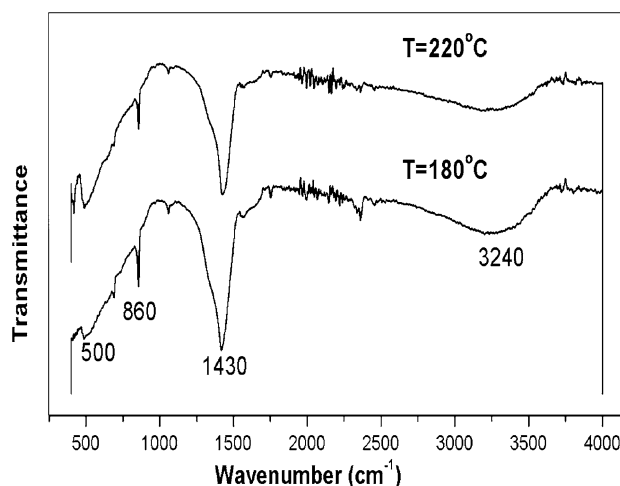
Fig. 3 Raman spectra of the as-prepared BaTiO$_3$ nanoparticles prepared by CHM approach at processing temperatures: 180, 220 and 250 °C

Fig. 4 FT-IR spectra of the as-prepared BaTiO$_3$ nanoparticles prepared via CHM method at 180 and 220 °C growth temperatures

however, Raman active modes are expected for the non-centrosymmetric tetragonal phase structure. In the literature, Raman activity of the cubic phase has been generally attributed to disorder of titanium in the nominally cubic phase. The Raman spectrum of the prepared nanoparticles at room temperature shows phonon bands at $\sim$492 [E, A1 (TO)] and 720 cm^{-1} [A1, E (LO)]. In addition to an intense non-Gaussian broadband about at $\sim$230 cm^{-1} [B1, E (TO)], all of the peaks suggest characteristics Raman active modes for the tetragonal phase local structure (Fig. 3) [18, 19]. On the other hand, Raman results of BT nanoparticles prepared at 220 and 250 °C reveal a relatively sharp bands around 492 [A1, E (TO)] and 720 cm^{-1} [A1, E (LO)]. Figure 3 also shows a small peak at 1054 cm^{-1} appears in both the spectra for the samples prepared at 180 and 220 °C, which could be the impurity peak not detected by the XRD due to its less sensitivity compared to Raman spectroscopy [20]. This impurity peak cannot be seen for the sample prepared at 250 °C, which signifies the processing temperature for the chemical reaction and subsequently for the purity of the obtained product. No peak exists in the region of low wave number below 200 cm^{-1} which could be expected for the BaCl$_2$ salt and manifests the formation of salt-free BT nanoparticles.

3.3 FT-IR analysis

In order to investigate the chemical nature, impurities and chemical bonding of the BT product, the IR spectra are taken in the region of our interest. Figure 4 shows FT-IR spectra of BT nanoparticles synthesized at 180 and 220 °C for constant reaction time of 48 h. The broadband between

2800 and 3600 cm^{-1} indicates the presence of H$_2$O and OH groups (or the OH^{-1}) in the product. Furthermore, the small peaks which appear at 860 and 500 cm^{-1} correspond to Ti–O stretching bands of the BaTiO$_3$ nanostructures [21]. Similarly, the peak at 1430 cm^{-1} is attributed to the symmetric stretching vibrations of carboxylic groups [21, 22]. These results reveal that impurities such as H$_2$O, hydroxyl and carboxylic groups decrease for BT nanoparticles at 220 °C. The sample at 250 °C shows a similar behavior not shown here.

3.4 Scanning electron microscopy (SEM)

The SEM micrographs of the BaTiO$_3$ nanostructures prepared at 180, 220 and 250 °C are given in Fig. 5a, b, c, d. These micrographs have low aggregation and narrow particle size distribution with a mean diameter in the range of 97–250 nm. The SEM micrographs reveal cuboid shape BT. From the cross-sectional view of SEM images, it is clear that at 180 °C, a very small number of cuboids are formed with a large number of amorphous products. But amorphous nature of the nanocuboids nearly disappears at 220 °C, which agrees with the strong peak in the XRD pattern. Interesting transition from cuboids into spherical ball-like nanostructure is obtained at higher synthesis temperature of 250 °C. The cubic-like nature of BT nanoparticles and the improved crystallinity with synthesis temperature have also been confirmed by the XRD pattern. The chemical compositions of the nanocuboids have been examined by energy-dispersive X-ray spectroscopy (EDX) [Fig. 5d]. The obtained EDS spectrum clearly indicates Ba, Ti and O elements in the product.
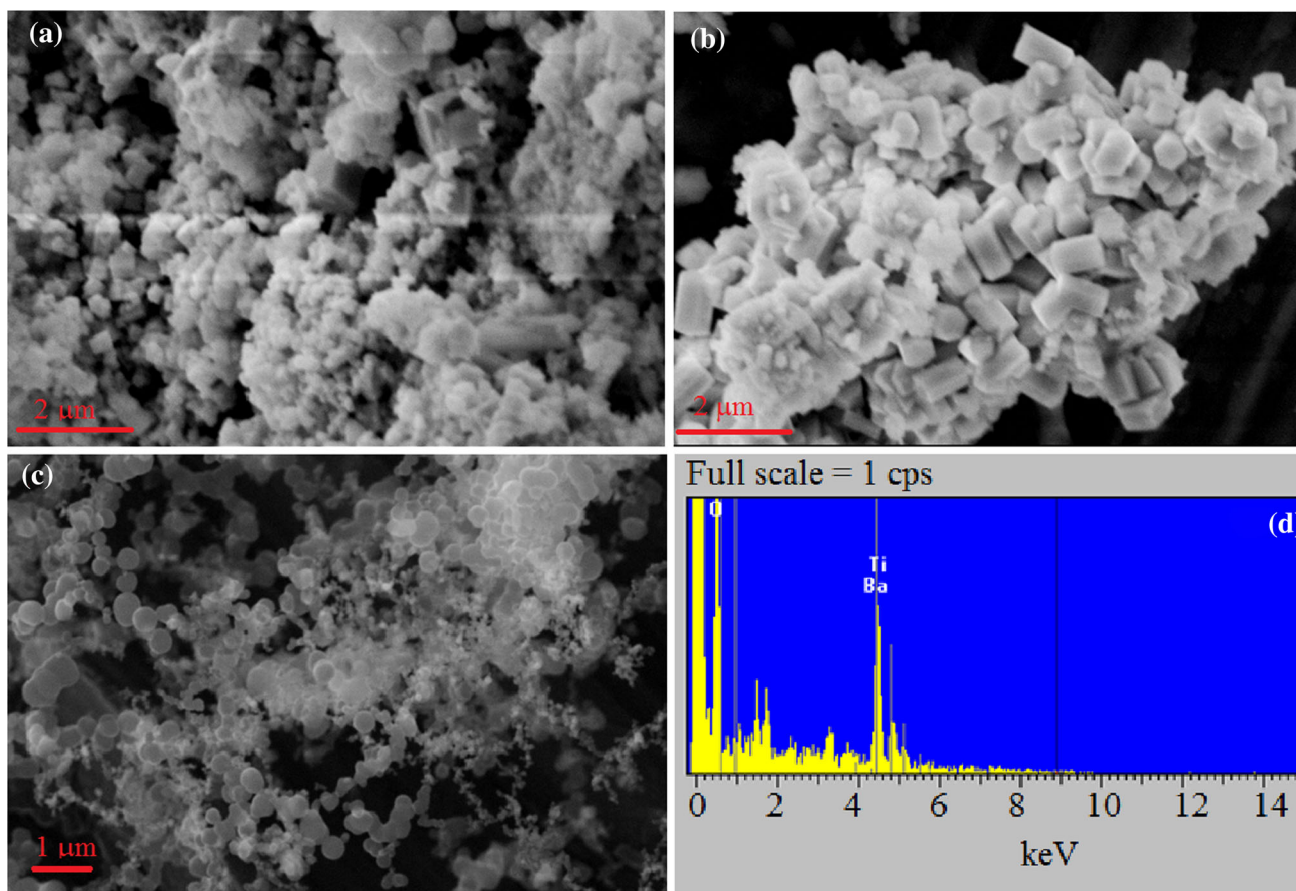
Fig. 5 SEM images of the as-prepared BaTiO₃ nanoparticles synthesized by CHM method at **a** 180, **b** 220 and **c** 250 °C process temperatures **d** EDS spectra of the BaTiO₃ nanoparticles prepared at 220 °C

4 Conclusion

In summary, a low-temperature and low-cost CHM synthesis method was applied for the preparation of BT nanomaterials (nanocuboids, nanoparticles) and successfully demonstrated. Particle size manipulation, surface smoothness, composition and crystal structure of these nanostructures strongly depend on the process temperature. The prepared product BT is polycrystalline in nature with cubic crystal structure. The crystallinity and cubic nature were improved with synthesis temperatures at 220 and 250 °C. A morphological structural transition from cuboids into spherical ball-shaped particles was observed. FT-IR spectra revealed that increasing the reaction temperature will induce a decrease in the hydroxyl ions due to water molecules in the BT product. The phonon bands in the Raman spectra indicated a local tetragonal distortion in the crystal structure. Although XRD results reported cubic structure, but the observed Raman active modes suggested a certain degree of tetragonality on the atomic scale. From the SEM results, we concluded that the BT nanoparticles were nanocuboids and spherical shaped nanoparticles.

These results indicate that the method of CHM can be used to produce complex nanomaterials for high-tech optoelectronic applications.

References

1. M.E. Lines, A.M. Glass, *Principles and Applications of Ferro-electrics and Related Materials* (Clarendon Press, Oxford, 1977)
2. S.-T. Huang, W.W. Lee, J.-L. Chang, W.-S. Huang, S.-Y. Chou, C.-C. Chen, J. Taiwan Inst. Chem. Eng. **45**(4), 1927–1936 (2014)
3. J. Miao, C. Hu, H. Liu, Y. Xiong, Mater. Lett. **62**, 235–238 (2008)
4. W.W. Lee, C.-S. Lu, C.-W. Chuang, Y.-J. Chen, J.-Y. Fu, C.-W. Siao, C.-C. Chen, RSC Adv. **5**, 23450–23463 (2015)
5. Y.-R. Jiang, S.-Y. Chou, J.-L. Chang, S.-T. Huang, H.-P. Lin, C.-C. Chen, RSC Adv. **5**, 30851–30860 (2015)
6. X.H. Zhu, J.M. Zhu, S.H. Zhou, Z.G. Liu, N.B. Ming, D. Hesse, Solid State Phenom. **106**, 41–46 (2005)

7. U. Manzoor, D.K. Kim, J. Mater. Sci. Technol. **23**, 655–658 (2007)

8. W.W. Lee, W.-H. Chung, W.-S. Huang, W.-C. Lin, W.-Y. Lin, Y.-R. Jiang, C.-C. Chen, J. Taiwan Inst. Chem. Eng. **44**(4), 660–669 (2013)

9. J.-H. Park, D.H. Yoo, B.K. Moon, G.-J. Jung, J. Korean Phys. Soc. **49**, S680–S683 (2006)

10. T.M. Khan, T. Shahid, M. Zakria, R.I. Shakoor, J Electron Mater Lett **11**, 366–373 (2015)

11. T.M. Khan, M. Zakria, R.I. Shakoor, M. Ahmad, M. Raffi, Advanced Materials Lett **6**, 592–599 (2015)

12. C. Hu, Y. Xi, H. Liu, Z.L. Wang, J. Mater. Chem. **19**, 858–868 (2009)

13. J. Miao, C. Hu, H. Liu, Y. Xiong, Mater. Lett. **62**, 235–238 (2008)

14. R.L. Brutchey, D.E. Morse, Angew. Chem. Int. Ed. **45**, 6564–6566 (2006)

15. M.R.A. Bhuiyan, M.M. Alam, M.A. Momin, M.J. Uddin, M. Islam, Int. J. Mater. Mech. Eng. **1**, 21–24 (2012)

16. Y. Mao, S. Mao, Z.-G. Ye, Z. Xie, L. Zheng, Mater. Chem. Phys. **124**, 1232–1238 (2010)

17. M.B. Smith, K. Page, T. Siegrist, P.L. Redmond, E.C. Walter, R. Seshadri, L.E. Brus, M.L. Steigerwald, J. Am. Chem. Soc. **130**, 6955–6963 (2008)

18. M. El Marssi, F. Le Marrec, I.A. Lukyanchuk, M.G. Karkut, J. Appl. Phys. **94**, 3307–3312 (2003)

19. G. Busca, G. Ramis, J.M. Gallardo Amores, V. Sanchez Escribano, P. Piaggio, J. Chem. Soc. Faraday Trans. **90**, 3181–3190 (1994)

20. M.L. Moreira, G.P. Mambrini, D.P. Volanti, E.R. Leite, M.O. Orlandi, P.S. Pizani, V.R. Mastelaro, E. Longo, J.A. Varela, Chem. Mater. **20**, 5381–5387 (2008)

21. E.A. Stefanescu, X. Tan, Z. Lin, N. Bowler, M.R. Kessler, Polymer **52**, 2016–2024 (2011)

22. X. Wei, G. Xu, Z. Ren, G. Shen, G. Han, J. Am. Ceram. Soc. **91**, 3774–3780 (2008)